

TM Electromagnetic Scattering from Multilayered Dielectric Bodies – Numerical Solution

F. Seydou^{1,2}, *R. Duraiswami*², *N.A. Gumerov*² & *T. Seppänen*¹

1. Department of Electrical and Information Engineering University of Oulu, P.O. Box 3000, 90401 Finland
2. Institute for Advanced Computer Studies University of Maryland, College Park, MD

Abstract

An integral equation approach is derived for an electromagnetic scattering from an M multilayered dielectric domain. The integral equation is valid for $2D$ and $3D$ Helmholtz equation. Here we show the numerical solution for the $2D$ case by using the Nyström method. For validating the method we develop a mode matching method for the case when the domains are multilayered circular cylinders and give numerical results for illustrating the algorithm.

Introduction

Problems in layered media are of significant importance in many areas of technology (cf. [1] and the references therein). In this paper we discuss some analytical and computational results for the problem of approximating the scattered electromagnetic field from M layered two-dimensional scatterer. The scatterer is a nested body consisting of a finite number of homogeneous layers (annular regions) with boundary conditions on the interfaces. The straightforward way for solving this type of problems via boundary element methods is by using Green's theorem in each domain [1]. Another alternative is to consider the use of single and/or double layer potentials [2]. In the case of one interface, both methods yield a single integral equation for a single unknown if the interface is impenetrable (e.g. impedance core). However, when the body is penetrable with one interface (e.g. dielectric core), they lead to a pair of integral equations for a pair of unknowns [2]. We deduce that, by using these approaches in the multilayered dielectric domain, for N interfaces we have $2N$ unknown functions to determine. From a computational point of view, it is highly desirable to obtain less equations and less unknowns. In the case of one interface, the so called transmission problem, one integral equation involving one unknown was obtained by a few authors (see [5] and the references therein). The purpose of this paper is to obtain a single integral equation on each interface for the multilayered domain case. In [5] the transmission problem was studied and a single integral equation for one unknown was obtained by using a hybrid of Green's theorem and layer potentials. Here we alternate the layer potentials and Green's theorems in the multilayered domain. We implement numerical computations using the Nyström method. Our results are validated by developing a mode matching approach for the case of a multilayered circular cylinder and compare the two algorithms.

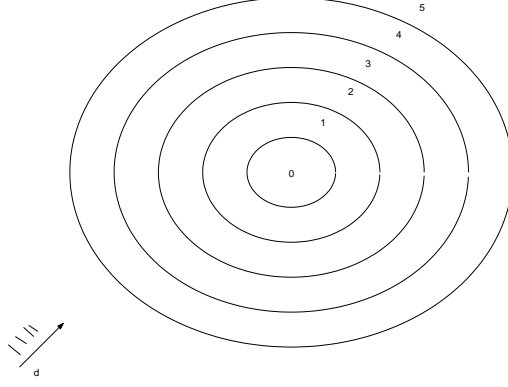


Figure 1: The geometry for the case of five circular concentric layered cylinders

1 The mathematical formulation of the problem

To fix ideas let us consider the $2D$ case. Let \mathbf{D}_l , $l = 0, 1, \dots, M-1$ be M bounded domains in \mathbf{R}^2 such that $\overline{\mathbf{D}}_{l-1} \subset \mathbf{D}_l$, $l = 1, 2, \dots, M-1$. Let Γ_l be the C^2 boundaries of \mathbf{D}_{l-1} , $l = 1, \dots, M$. Now let $\Omega_1 = \mathbf{D}_0$, $\Omega_l = \mathbf{D}_l \setminus \overline{\mathbf{D}}_{l-1}$, $l = 1, \dots, M-1$, and $\Omega_M = \mathbf{R}^2 \setminus \overline{\mathbf{D}}_{M-1}$. We assume that Ω_M is simply connected. See Figure 1 for Ω_l , $l = 0, 1, \dots, 5$. This is a special case of the general geometry where we have ($M = 5$) circular concentric cylinders that are infinite in length and their axes are parallel to the z direction.

Each of the regions Ω_l is a dielectric material of complex permittivity and permeability ϵ_l and μ_l ($l = 0, \dots, M$), respectively. This geometry is illuminated by an incident field which is a plane wave with direction $\mathbf{d} = (\cos \phi_0, \sin \phi_0)$.

It can be shown that we have to solve the following type of boundary value problem for the Helmholtz equation.

$$(\Delta + \kappa_l^2)u_l = 0 \quad \text{in } \Omega_l, \quad l = 0, \dots, M,$$

where the wave numbers κ_l are given by $\kappa_l = \omega \sqrt{\epsilon_l \mu_l}$, ω is the frequency, with the following continuity conditions on the internal interfaces:

$$\frac{\partial}{\partial \nu} u_l = \rho_l \frac{\partial}{\partial \nu} u_{l-1} \quad \text{on } \Gamma_l, \quad l = 1, \dots, M-1,$$

$$u_l = u_{l-1} \quad \text{on } \Gamma_l, \quad l = 1, \dots, M-1,$$

with $\rho_l = \frac{\hat{\rho}_l}{\hat{\rho}_{l-1}}$, $l = 1, 2, \dots, M$, where $\hat{\rho}_l = \sqrt{\frac{\mu_l}{\epsilon_l}}$ is the intrinsic impedance.

On the outermost interface we have

$$\frac{\partial u}{\partial \nu} = \rho_M \frac{\partial}{\partial \nu} u_{M-1} \quad \text{on } \Gamma_M,$$

$$u = u_{M-1} \quad \text{on } \Gamma_M,$$

where,

$$u = u_M + u^i \quad \text{in } \Omega_M$$

and the given incident field, u^i , satisfies

$$\Delta u^i + \kappa_M^2 u^i = 0$$

everywhere. In addition, u_M must satisfy the Sommerfeld radiation condition, i.e.,

$$\lim_{|\mathbf{x}| \rightarrow \infty} |\mathbf{x}|^{1/2} \left(\frac{\partial u_M}{\partial |\mathbf{x}|} - i\kappa_M u_M \right) = 0.$$

The unit outward normal ν to Γ_l is assumed to be directed towards the exterior domain. The above problem is known as the TM mode. The TE mode is obtained by replacing ρ_l by $\frac{1}{\rho_l}$. We denote the fundamental solution to the Helmholtz equations (the free-space source) by

$$\Phi_k(\mathbf{x}, \mathbf{y}) = -\frac{i}{2} H_0^{(1)}(\kappa_k |\mathbf{x} - \mathbf{y}|), \quad k = 0, 1, \dots, M,$$

where $H_0^{(1)}$ is the Hankel function of the first kind and order zero. Throughout this paper i will denote the complex constant satisfying $i^2 = -1$.

2 The integral equation approach

First, for non zero functions ϕ_l , $l = 1, 2, \dots, M$, define the single and double layer potentials as

$$S_k^l \phi_l(\mathbf{x}) = \int_{\Gamma_l} \Phi_k(\mathbf{x}, \mathbf{y}) \phi_l(\mathbf{y}) ds(\mathbf{y}), \quad \mathbf{x} \in \mathbf{R}^2 \setminus \Gamma_l,$$

and

$$D_k^l \phi_l(\mathbf{x}) = \int_{\Gamma_l} \frac{\partial}{\partial \nu_l(\mathbf{y})} \Phi_k(\mathbf{x}, \mathbf{y}) \phi_l(\mathbf{y}) ds(\mathbf{y}), \quad \mathbf{x} \in \mathbf{R}^2 \setminus \Gamma_l,$$

respectively, for $k = 0, 1, \dots, M$. Their normal derivatives are denoted by P_k^l and Q_k^l , respectively, for $k = 0, 1, \dots, M$.

We have the continuity relations

$$S_k^l = \hat{S}_k^l, \quad Q_k^l = \hat{Q}_k^l,$$

and the jump relations

$$D_k^l = \mp I + \hat{D}_k^l \quad \text{and} \quad P_k^l = \pm I + \hat{P}_k^l,$$

where, the upper (lower) sign corresponds to the limit when \mathbf{x} approaches Γ_l from the outside (inside). The hat on each operator represents it on the boundary Γ_l .

To arrive at the desired integral equation we define a layer ansatz by $E_k^l = D_k^l - i\eta_l S_k^l$ for $l \neq 0$ and $E_k^0 = 0$ (with normal derivative H_k^l) in Ω_l , where η_l s are complex constants chosen to obtain well-posedness, $l = 0, 2, 4, \dots$, and Green's theorem in $\Omega_{l'}$, $l' = 1, 3, 5, \dots$. In particular, let us assume that M is odd. Then, in the core region Ω_0 we define

$$u_0(\mathbf{x}) = E_0^1 \phi_1(\mathbf{x}), \quad \mathbf{x} \in \Omega_0. \quad (2.1)$$

In the outermost domain, we use Green's theorem ([2] pp. 68-70) to obtain

$$\begin{cases} 2u_M(\mathbf{x}) = S_M^M \frac{\partial}{\partial \nu} u(\mathbf{x}) - D_M^M u(\mathbf{x}), & \mathbf{x} \in \Omega_M, \\ -2u^i(\mathbf{x}) = S_M^M \frac{\partial}{\partial \nu} u(\mathbf{x}) - D_M^M u(\mathbf{x}), & \mathbf{x} \in \mathbf{R}^2 \setminus \overline{\Omega}_M. \end{cases} \quad (2.2)$$

In the other domains, for $l = 2, 4, \dots, M-1$, we define

$$u_l(\mathbf{x}) = E_l^l \phi_l(\mathbf{x}) + E_l^{l+1} \phi_{l+1}(\mathbf{x}), \quad \mathbf{x} \in \Omega_l, \quad (2.3)$$

and, using Green's theorem for $l = 1, 3, \dots, M - 2$ we have

$$\begin{cases} 2u_l(\mathbf{x}) = S_l^l \frac{\partial}{\partial \nu} u_l(\mathbf{x}) - S_l^{l+1} \frac{\partial}{\partial \nu} u_l(\mathbf{x}) - (D_l^l - D_l^{l+1})u_l(\mathbf{x}), & \mathbf{x} \in \Omega_l, \\ 0 = S_l^l \frac{\partial}{\partial \nu} u_l(\mathbf{x}) - S_l^{l+1} \frac{\partial}{\partial \nu} u_l(\mathbf{x}) - (D_l^l - D_l^{l+1})u_l(\mathbf{x}), & \mathbf{x} \in \mathbf{R}^2 \setminus \overline{\Omega}_l \end{cases} \quad (2.4)$$

Now, using the jump and continuity relations we obtain the second equation in (2.2) on Γ_M and the second equation in (2.4) on Γ_l and Γ_{l+1} ($l = 1, 3, 5, \dots, M - 2$). Using the boundary conditions, jump properties for the single and double layer potentials together with their derivatives, and replacing u_0 (given in (2.1)) and u_{l+1} (given in (2.3)) into these equations we arrive at a set of M integral equations with M unknowns ϕ_l on Γ_l , $l = 1, 2, \dots, M$. In particular, on Γ_M we have

$$-2u^i = \left(\rho_M \hat{S}_M^M H_{M-1}^{M-1, M} - (\hat{D}_M^M + I) \hat{E}_{M-1}^{M-1, M} \right) \phi_{M-1} + \left(\rho_M \hat{S}_M^M \hat{H}_{M-1}^M - (\hat{D}_M^M + I) \hat{E}_{M-1}^M \right) \phi_M,$$

and for l odd and less than M we have

$$0 = \left(\rho_l \hat{S}_l^l H_{l-1}^{l-1, l} + (\hat{D}_l^l - I) E_{l-1}^{l-1, l} \right) \phi_{l-1} + \left(\rho_l \hat{S}_l^l \hat{H}_{l-1}^l + (\hat{D}_l^l - I) \hat{E}_{l-1}^l \right) \phi_l + \left(\frac{1}{\rho_{l+1}} S_l^{l+1, l} \hat{H}_{l+1}^{l+1} + D_l^{l+1, l} \hat{E}_{l+1}^{l+1} \right) \phi_{l+1} + \left(\frac{1}{\rho_{l+1}} S_l^{l+1, l} H_{l+1}^{l+2, l+1} + D_l^{l+1, l} E_{l+1}^{l+2, l+1} \right) \phi_{l+2} \quad \text{on } \Gamma_l$$

$$0 = \left(\frac{1}{\rho_{l+1}} \hat{S}_l^{l+1} \hat{H}_{l+1}^{l+1} + (\hat{D}_l^{l+1} + I) \hat{E}_{l+1}^{l+1} \right) \phi_{l+1} + \left(\frac{1}{\rho_{l+1}} \hat{S}_l^{l+1} H_{l+1}^{l+2, l+1} + (\hat{D}_l^{l+1} + I) E_{l+1}^{l+2, l+1} \right) \phi_{l+2} \left(\rho_l S_l^{l, l+1} H_{l-1}^{l-1, l} + D_l^{l, l+1} E_{l-1}^{l-1, l} \right) \phi_{l-1} + \left(\rho_l S_l^{l, l+1} \hat{H}_{l-1}^{l, l} + D_l^{l, l+1} \hat{E}_{l-1}^{l, l} \right) \phi_l \quad \text{on } \Gamma_{l+1}$$

Remark: The above system is valid for the 3D Helmholtz equation.

3 Two dimensional validation

This section is devoted to the numerical solution of the above system and its validation for the 2D case. To this end, we use the Nyström method for the numerical solution and Bessel function expansion for the validation.

3.1 Discretization and numerical solution

The system is discretized using the Nyström method [3]. The resulting matrix equation, that involves matrix multiplications resulted from the multiplications of layer potentials and/or their derivatives, is solved by a standard LU decomposition approach. Let us note that the assumption that M is odd is not a lost of generality. In fact, for an even M we can use the same method, but for $M + 1$ regions, Γ_{M+1} encloses the scatterer, with $\kappa_{M+1} = \kappa_M$ and $\rho_{M+1} = 1$. This way has the advantage of keeping the same system of equations and the disadvantage of adding another equation and an unknown function ϕ_{M+1} . This may be overcome by starting with Green's theorem in the core region, alternate with layer ansatz and obtain the Green's theorem in Ω_M , which gives a different system than the previous argument.

3.2 The Mode Matching Approach

This method is studied in detail in [4]. Consider the case when the regions \mathbf{D}_l 's are circular cylinders with radii r_{l+1} and origins \mathbf{O}_{l+1} , $l = 0, 1, 2, \dots, M-1$; then we have the following expansions [1]: For the outermost region

$$u(\tilde{r}_M, \phi_M) = \sum_{n=-\infty}^{\infty} \left(b_n^M H_n^{(1)}(\kappa_M \tilde{r}_M) + J_n(\kappa_M \tilde{r}_M) \right) e^{-in(\phi_M - \phi_o)}$$

and for other regions we have

$$u_l(\tilde{r}_1, \phi_1) = \sum_{n=-\infty}^{\infty} \left(b_n^l H_n^{(1)}(\kappa_l \tilde{r}_1) + a_n^l J_n(\kappa_l \tilde{r}_1) \right) e^{-in(\phi_1 - \phi_o)}, \quad l = 0, 1, 2, \dots, M-1,$$

where $b_n^0 = 0$.

To enforce the boundary conditions we need the addition formula for u_l , $l = 1, \dots, M-1$ which means that the fields expressed in terms of $X_1 O_1 Y_1$ be translated to $X_l O_l Y_l$ coordinates. This yields

$$u_l(\tilde{r}_l, \phi_l) = \sum_{n=-\infty}^{\infty} \sum_{i=-\infty}^{\infty} J_{i-n}(\kappa_l d_{l1}) \left[b_n^l H_i^{(1)}(\kappa_l \tilde{r}_l) + a_n^l J_i(\kappa_l \tilde{r}_l) \right] e^{i(\phi_0 - (i-n)\phi_{l1})},$$

where d_{l1} is the distance between \mathbf{O}_1 and \mathbf{O}_l and ϕ_{l1} is the angle between $\mathbf{O}_1 \mathbf{O}_l$ and the x axis.

The sums in the above equations have to be truncated, at some number, N_0 , to obtain a finite system. Now we can use the expansions on the boundary together with their derivatives and the boundary conditions to obtain a linear system in the unknowns a_n^l and b_n^l . This system is also solved via LU decomposition approach.

3.3 Numerical Results

In this section, numerical solution obtained by using the integral equation (IE) and mode matching (MM) methods are presented. We have conducted several numerical experiments.

First we try to validate the MM method by analyzing the physical properties of the waves, by plotting the absolute values of the waves against the boundaries. To this end, we consider a cylinder with radius $r = 3$, so that we only have the inner and outermost domains, and keep the angle of the incident field $\phi_0 = 90$ deg and $\rho_1 = 1$ fixed. We would expect, for real κ_1 and complex κ_2 with negative imaginary part, the wave to diverge at the boundary. If, on the other hand, we have that the two wave numbers are real and equal, the absolute value of the wave should be unity. Finally, for the case when κ_1 is real and κ_2 is complex with a positive imaginary part, because of absorption, the absolute value of the wave must decay at the boundary and the bigger the imaginary part, the faster the wave should decay. Our numerical computations show that all these properties are satisfied, and the results are summarized in Figure 2.

Next we validated the IE method for one interface, centered at $\mathbf{O} = (-0.2, 0.7)$, by plotting the absolute value of the far field pattern (measured at a fixed observation point \hat{x}) against the incident angle for two different wave numbers using the IE and MM methods. See [3] for the definition of the far field pattern. The result is given in Figure 3, which shows a very good agreement of the two methods. Unless otherwise stated we used 32 grid points for the Nyström solver.

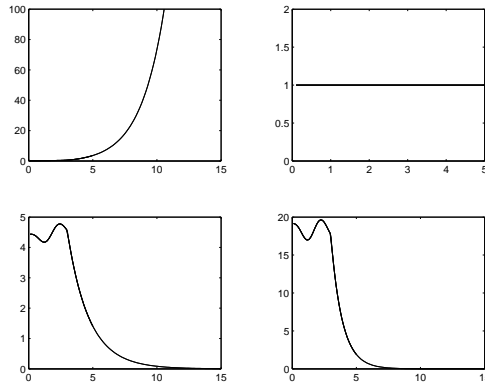


Figure 2: The case of one circular boundary ($r = 3$). The absolute value of the wave plotted against the radius. We have used $\kappa_1 = 2$ and $\kappa_2 = 2 - 0.5i$ (top left) $\kappa_1 = 2$ and $\kappa_2 = 2$ (top right), $\kappa_1 = 2$ and $\kappa_2 = 2 + 0.5i$ (bottom left), and $\kappa_1 = 2$ and $\kappa_2 = 2 + 4i$ (bottom right)

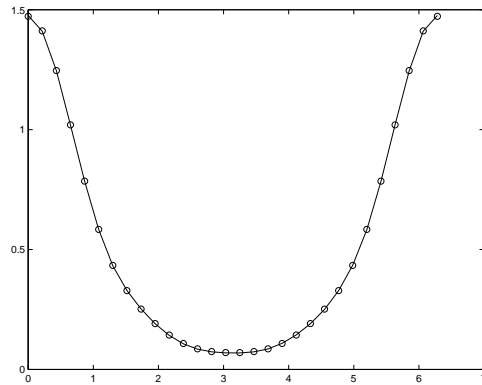


Figure 3: The absolute value of the far field pattern plotted against the incident angle using the MM ('o') and IE (solid line) methods. The case of one interface. We used $\kappa_0 = 2$, $\kappa_1 = 3$ and the radius is $r = 1$.

Our next examples are for the two and three-layered circular cases. First we plot the absolute value of the far field against the incidence angle for the two-layered case and then for the three-layered case. The results are shown in Figure 4 and Figure 5, respectively. In these cases as well we have very good agreements of the two methods.

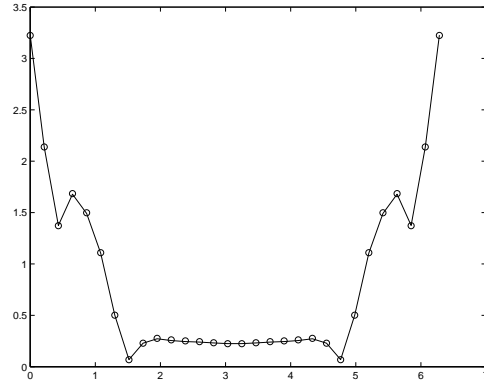


Figure 4: The absolute value of the far field pattern plotted against the incident angle using the MM ('o') and IE (solid line) methods. The case of two-layered circular cylinders. Here $\kappa_0 = 2$, $\kappa_1 = 3$, $\kappa_2 = 4$, $r_1 = 1$ and $r_2 = 2$.

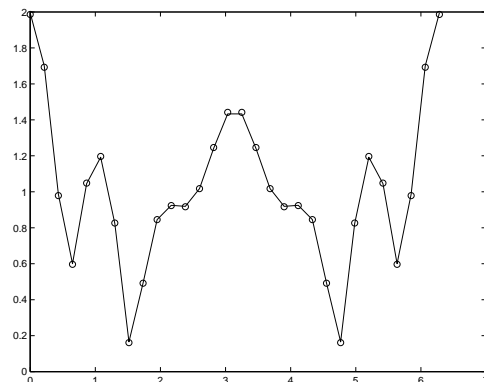


Figure 5: The absolute value of the far field pattern plotted against the incident angle for the MM ('o') and IE (solid line) methods. The case of three-layered circular cylinder. Here $\kappa_0 = 2$, $\kappa_1 = 3$, $\kappa_2 = 4$, $\kappa_3 = 1$, $r_1 = 1$, $r_2 = 2$ and $r_3 = 3$.

For the case of more circular layers we have the same conclusions, except that more grid points are needed, which is due to the errors in the computation of the layer potentials.

Our last example is for the case of three boundaries of kite type where MM method can not be performed (Figure 6). Here we investigate the convergence as well as the boundary conditions. For the former we compute the far field pattern for different wave numbers. The results are reported in the two tables below. We see clear convergence, and, as expected, it is fast. For the latter case we plot $|u_1|$ and $|u_2|$ on Γ_1 , $|u_2|$ and $|u_3|$ on Γ_2 , $|u_3|$ and $|u_4 + u^i|$ on Γ_3 , against the incident angle. From the boundary conditions we know that they must coincide. This is shown in Figures 7.

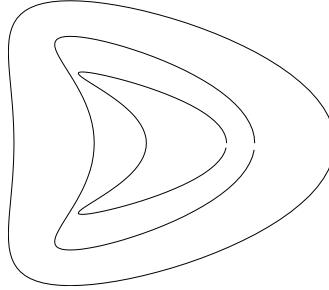


Figure 6: The geometry for the case of three boundaries of kite type.

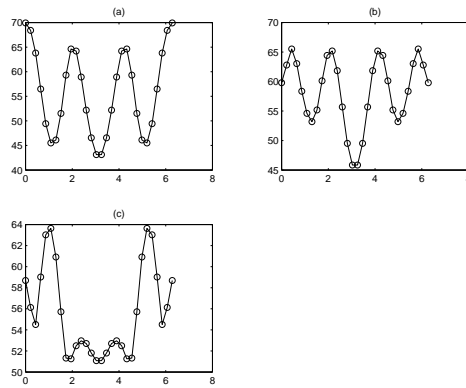


Figure 7: Here we plot $|u_j|$ ('o') and $|u_{j+1} + \frac{(j-1)(j-2)}{2}u^i|$ (solid line) on the boundary Γ_j against the incidence angle. In (a) we have the case $j=1$, in (b) $j=2$ and (c) $j=3$.

4 Conclusion and future work

We have developed an integral equation approach for solving the M multilayered electromagnetic problem and used the Nyström method for the numerical computation. The algorithm was validated by a Fourier expansion method for circular (not necessarily concentric) cylinders. One may think as a disadvantage for our method the numerous matrix vector multiplications. This problem can be overcome by using fast multiple methods where these operations are done very quickly. Our results also show the (expected) fast convergence of Nyström method for analytic boundaries. The natural expansion of our method is for the numerical solution of the three-dimensional electromagnetic problem, and to the case of multiple scatterers.

Table 1: Parameter values and description for the geometry in Figure 6.

Description	Symbol	Data 1	Data 2	Data 3
Wave numbers	κ_0	2	4	1+i
	κ_1	3	5	2
	κ_2	1.5	4.5	2+0.5i
	κ_3	2.5	5.5	3

Table 2: The numerical results using the integral equation (IE) approach . The data are given in Table 1. The number N is the number of Nyström points.

	N	IE
Data 1	8	$-3.1863 + 0.4213i$
	16	$-3.5238 + 0.1952i$
	32	$-3.5215 + 0.1955i$
	64	$-3.5214 + 0.1954i$
Data 2	8	$-11.9843 + 15.8975i$
	16	$-3.5291 + 3.2993i$
	32	$-4.2103 + 3.5349i$
	64	$-4.2103 + 3.5344i$
Data 3	8	$-2.3889 + 1.6002i$
	16	$-2.5120 + 1.5746i$
	32	$-2.5126 + 1.5739i$
	64	$2.5126 + 1.5739i$

References

- [1] W. C. Chew, 1990. *Waves and Fields in Inhomogeneous Media*. Van Nostrand Reinhold
- [2] D. Colton and R. Kress, 1983. *Integral Equation in Scattering Theory*. John Wiley & Sons.
- [3] D. Colton and R. Kress, 1992. *Inverse Acoustic and Electromagnetic Scattering Theory* (Springer Verlag).
- [4] A. Kishk, R. Parrikar & A. Elsherbeni, 1992. Electromagnetic Scattering from an eccentric multilayered circular cylinder. *IEEE Trans. Antennas and Prop.* Vol. 40, No3 pp. 295-303
- [5] Kleinmann, R.E. Martin, P.A., 1988 On single integral equations for the transmission problem of acoustics. *SIAM J. Appl. Math.* 48, No.2, 307-325.